

Fabrication and Characterization of Nitinol-Copper Shape Memory Alloy Bimorph Actuators

E. Wongweerayoot, W. Srituravanich, and A. Pimpin

(Submitted August 19, 2014; in revised form October 23, 2014; published online December 2, 2014)

This study aims to examine the effect of annealing conditions on nitinol (NiTi) characteristics and applies this knowledge to fabricate a NiTi-copper shape memory alloy bimorph actuator. The effect of the annealing conditions was investigated at various temperatures, i.e., 500, 600, and 650 °C, for 30 min. With the characterizations using x-ray diffraction, energy dispersive spectroscopy, and differential scanning calorimetry techniques, the results showed that annealing temperatures at 600 and 650 °C were able to appropriately form the crystalline structure of NiTi. However, at these high annealing temperatures, the oxide on a surface was unavoidable. In the fabrication of actuator, the annealing at 650 °C for 30 min was chosen, and it was performed at two pre-stressing conditions, i.e., straight and curved molds. From static and dynamic response experiments, the results suggested that the annealing temperature significantly affected the deflection of the actuator. On the other hand, the effect of pre-stressing conditions was relatively small. Furthermore, the micro gripper consisting of two NiTi-copper bimorph actuators successfully demonstrated for the viability of small object manipulation as the gripper was able to grasp and hold a small plastic ball with its weight of around 0.5 mg.

Keywords annealing temperature, bimorph, copper, differential scanning calorimetry, energy dispersive spectroscopy, micro actuator, micro fabrication, nitinol, shape memory alloy, x-ray diffraction

1. Introduction

For three decades, several actuation mechanisms have been proposed for micro electro-mechanical systems (MEMS). One powerful mechanism is the shape memory effect of alloy materials since this mechanism has an ability to recover large transformation when it is heated and cooled. Among various shape memory alloy (SMA) materials, nickel-titanium, or nitinol (NiTi), is especially attractive due to its low-operating temperature, large deflection, and actuating force (Ref 1-10). For the integration into microsystems, shape memory materials in thin-film form are extensively studied. The main challenge in the development of shape memory thin films has been the control of the microstructure including stoichiometry and precipitates. In addition, the importance of thin film SMA actuators has further increased with the number of applications that have been developed with SMAs in microsystems. For example, Makino et al. (Ref 11) as well as Sassa et al. (Ref 12) created a micropump, Takeuchi and Shimoyama (Ref 13), Gill et al. (Ref 14) as well as Fu et al. (Ref 15) created a microgripper, and Chung and Chan (Ref 16) created a micro mechanism for an imaging sensor.

The fabrication of NiTi alloy thin film mainly consists of two important processes, i.e., sputtering deposition and post-sputtering annealing. The sputtering deposition is a typical technique to create a thin film of Ni-Ti. For the post-sputtering annealing, it is a process to form NiTi alloy microstructures and especially customize the material's properties that consequently affects a microsystem's performance. The annealing process is performed at high temperature (normally over 450 °C) to form a crystalline structure of NiTi, e.g., martensite, austenite, and R-phase. The annealing is typically performed by heating an as-deposited Ni-Ti thin film in a high vacuum furnace (Ref 11, 15, 16). However, there are several other possibilities for annealing such as heating by high-power laser (Ref 17), heating by halogen lamp (Ref 18), and heating in a quartz tube furnace with inert gas overflow (Ref 12).

In this research, a micro bimorph actuator with NiTi alloy and copper (Cu) has been developed using a new fabrication technique. With this combination of two materials, the laminated structure bends due to the mismatch of strain between the two materials when the structure is heated or cooled. The proposed fabrication technique was successfully employed for micro thermal bimorph actuators in previous work (Ref 19). It starts by initially forming a freestanding copper structure by the electroplating technique to deposit copper on a stainless substrate between photoresist molds. After achieving the desired thickness, the photoresist mold is removed using sodium hydroxide solution to release the copper structure. Consequently, a Ni-Ti thin film is deposited on the freestanding copper structure by the sputtering technique, and the annealing is then performed at a high temperature in a quartz tube furnace with argon overflow to form NiTi alloy microstructure. Figure 1 shows a schematic drawing of the proposed fabrication process.

As mentioned earlier, the post-sputtering annealing significantly affects the material performance. However, the information about the annealing of Ni-Ti thin film on a copper

E. Wongweerayoot, W. Srituravanich, and A. Pimpin, Department of Mechanical Engineering, Faculty of Engineering, Chulalongkorn University, Phayathai Road, Patumwan, Bangkok 10330, Thailand. Contact e-mail: alongkorn.p@chula.ac.th.

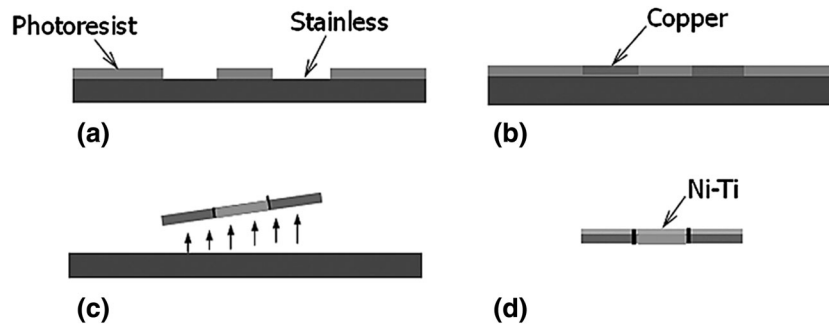


Fig. 1 Proposed fabrication process for a SMA bimorph actuator: (a) patterning a mold with photolithography technique on a stainless plate, (b) electroplating copper, (c) removing photoresist mold, (d) sputtering Ni-Ti thin film on the freestanding copper structure

structure as employed is still limited. Therefore, the effect of annealing parameters, i.e., temperature and pre-stressing, on the material performance was investigated in this study. Characterization of the Ni-Ti thin film on the copper structure under different conditions was performed using x-ray diffraction (XRD), energy dispersive spectroscopy (EDS), and differential scanning calorimetry (DSC) techniques. At the end, the performance of the SMA NiTi-copper bimorph actuator, annealed at different pre-stressing conditions, was examined.

2. Sample Preparation

In this study, the preparation of as-deposited Ni-Ti thin film was done on both previously prepared 12- μm thick freestanding copper structure and silicon substrate by the sputtering technique, as silicon substrate is a typical substrate material for alloy characterization due to its thermal stability and chemical inertness as commonly found in the literature (Ref 20-22). The Ni-Ti thin film was deposited by DC magnetron sputtering on both types of sample using a NiTi target with the ratio between Ni to Ti equal to 1.0. The base pressure in the deposition after filling argon was set at 3×10^{-3} mbar, and the DC power was controlled at a current of 0.2 A. At these conditions, the Ni-Ti film was deposited at a rate of 1 $\mu\text{m}/\text{hour}$ until its thickness was around 5 μm .

Afterward, the Ni-Ti thin film on both types of sample was annealed in the quartz tube furnace, whose schematic setup is shown in Fig. 2, to form a NiTi alloy microstructure. Firstly, air inside the quartz tube was removed by a vacuum pump. After turning off the vacuum pump, argon was circulated in order to force oxygen out from the quartz tube. This process was repeated three times before turning on a heater. To prevent oxidation, argon overflow was employed during the annealing process. The heater was controlled at a heating rate of 10 $^{\circ}\text{C}/\text{min}$. At a desired annealing temperature, the temperature was held constant for 30 min. After that, the heater was turned off resulting in a natural cooling for 3-4 h with an average cooling rate of around 3 $^{\circ}\text{C}/\text{min}$. In this study, the desired annealing temperature was varied as 500, 600, and 650 $^{\circ}\text{C}$.

3. Material Characterization

Figure 3(a) and (b), respectively, show XRD results of as-deposited Ni-Ti thin film on a copper structure and a silicon

substrate, compared to those with annealing at various temperatures. In this study, XRD analysis was done at room temperature. In both types of samples, for the as-deposited structure and that with annealing at 500 $^{\circ}\text{C}$, the results did not exhibit any peak except for Cu at 2θ of 43.2 $^{\circ}$. For the structure with annealing at 600 and 650 $^{\circ}\text{C}$, the results exhibited the peak of austenite phase of NiTi (110) at 2θ of 42.5 $^{\circ}$. Moreover, at these high annealing temperatures, the XRD pattern showed the presence of other peaks corresponding to Ni-rich precipitates, which were identified as Ni₃Ti. The evolution of Ni-rich precipitates may be due to holding for long duration at high temperature after annealing. In addition, it was also observed that the XRD results of Ni-Ti thin film on the copper structure exhibited the peak of NiCu alloy structure at 2θ of 44 $^{\circ}$. One possibility that resulted in the formation of NiCu alloy was the diffusion of either nickel or copper across their boundary to form the NiCu alloy structure. The results suggested that the crystalline structure of NiTi alloy film became better oriented when the annealing temperature was higher, and it also resulted in the presence of austenite phase even at room temperature. Moreover, the significant effect of annealing at 650 $^{\circ}\text{C}$ was observed so that the examination of the Ni-Ti thin films, which were annealed at 650 $^{\circ}\text{C}$, was performed more extensively, as discussed in the next section.

The composition of the Ni-Ti thin films before and after annealing was examined using the EDS technique. The results comparing two conditions, i.e., as-deposited Ni-Ti film and that with annealing at 650 $^{\circ}\text{C}$ for 30 min, on a copper structure are, respectively, shown in Fig. 4(a) and (b). With this technique, the near-surface material shallower than 1 μm from its surface was examined. Firstly, after annealing at 650 $^{\circ}\text{C}$, oxygen was significantly observed, which suggested that the oxidation on the film surface was not avoidable with the argon overflow technique as desired. After examining at three locations over the top surface of each type of sample, the average composition of Ni-Ti thin film excluding oxygen content obtained from the EDS results was calculated. The average composition in the near-surface layer of the as-deposited Ni-Ti thin film on a copper structure and silicon substrate was approximately the same at 39.3 wt.%-Ti and 60.7 wt.%-Ni. After annealing at 650 $^{\circ}\text{C}$ for 30 min, the average Ni and Ti composition of the film on the copper structure and silicon substrate was, respectively, transformed to 51.9 wt.%-Ti, 48.1 wt.%-Ni, and 62.4 wt.%-Ti, 37.6 wt.%-Ni. Obviously from the results, Ni and Ti contents in the near-surface layer of Ni-Ti thin film on both structures had transformed drastically. This was likely due to the formation of TiO₂ film over the surface that resulted in a

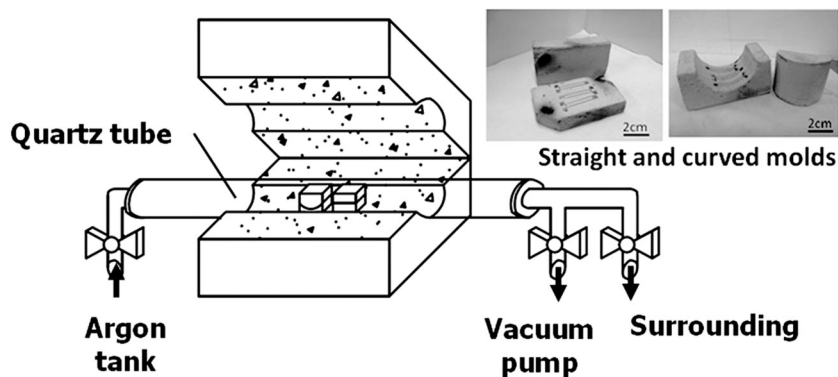


Fig. 2 Schematic setup of quartz tube furnace with argon overflow

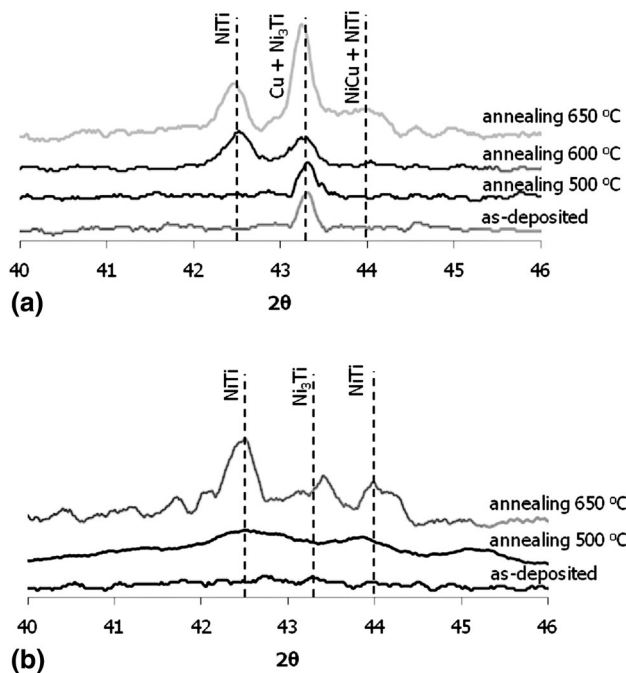


Fig. 3 XRD results of Ni-Ti thin film at various annealing temperatures: (a) Ni-Ti thin film on a copper structure, (b) Ni-Ti thin film on a silicon substrate

significant decreasing of Ni content compared to Ti in the near-surface layer of the thin film (Ref 23-25). In addition, the occurrence of the oxide was not uniform as a deviation of composition around ± 4 wt.% was obtained after high temperature annealing.

In this study, the attempt to vertically cut the thin film for cross-section examination was not successful due to the distortion of thin-film material during a cutting process. Thus, only the examination on the side-wall of the thin film was performed. Figure 5(a)-(d) show EDS results on the side wall of as-deposited Ni-Ti thin film on the copper structure compared to that with annealing at 650 °C for 30 min. In Fig. 5(b), the formation of TiO_2 is observed in a spherical shape with the grain size of around 200-300 nm on the Ni-Ti film surface after the annealing. This phenomenon has been commonly reported in literature (Ref 25). Figure 5(c) shows that the Ni to Ti ratio of the as-deposited Ni-Ti film was almost

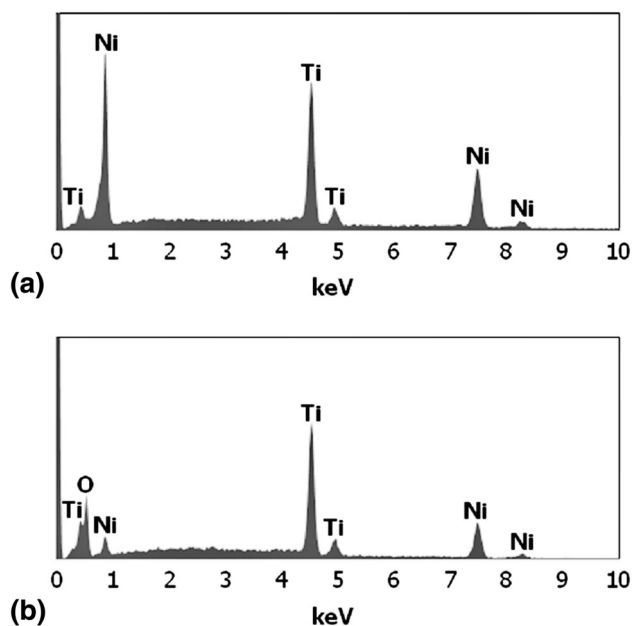


Fig. 4 EDS results for near-surface layer on a top surface of Ni-Ti thin film on a copper structure: (a) as-deposited, (b) with annealing at 650 °C for 30 min

constant throughout the thickness of the thin film. Furthermore, a relatively significant percentage of oxygen was observed due to natural oxidation that occurred on the structure surface during the experiments. After the annealing, the composition in the near-surface layer was changed as shown in Fig. 5(d). The percentage by weight of Ni reduced and became much lower than that of Ti likely due to the formation of TiO_2 in the near-surface layer as mentioned earlier. Moreover, the Cu content increased significantly at the positions located in the Ni-Ti thin film. This result suggests that copper diffused into the Ni-Ti thin film during the annealing process, which agreed with the XRD results.

The transformation behavior during heating and cooling at the rate of 15 °C/min was investigated using the DSC technique. A special technique to prepare pure as-deposited Ni-Ti thin film was employed. The as-deposited Ni-Ti thin film was prepared by initially sputtering Ni-Ti thin film on a glass slide. After breaking the glass slide, the Ni-Ti film was peeled off easily. The peeled off Ni-Ti thin film was annealed with the

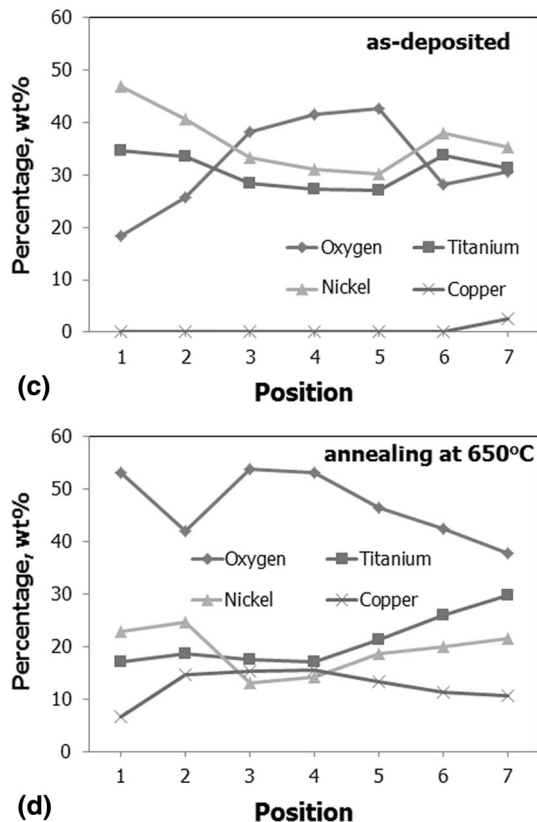
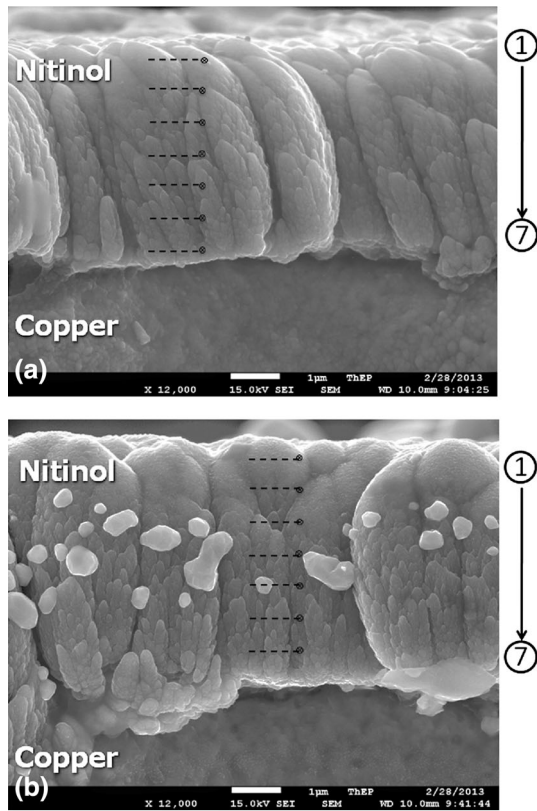


Fig. 5 EDS results for near-surface layer on a side wall of Ni-Ti thin film on a copper structure: (a) image of as-deposited film, (b) image after annealing at 650 °C for 30 min, (c) composition of as-deposited film, (d) composition after annealing at 650 °C for 30 min

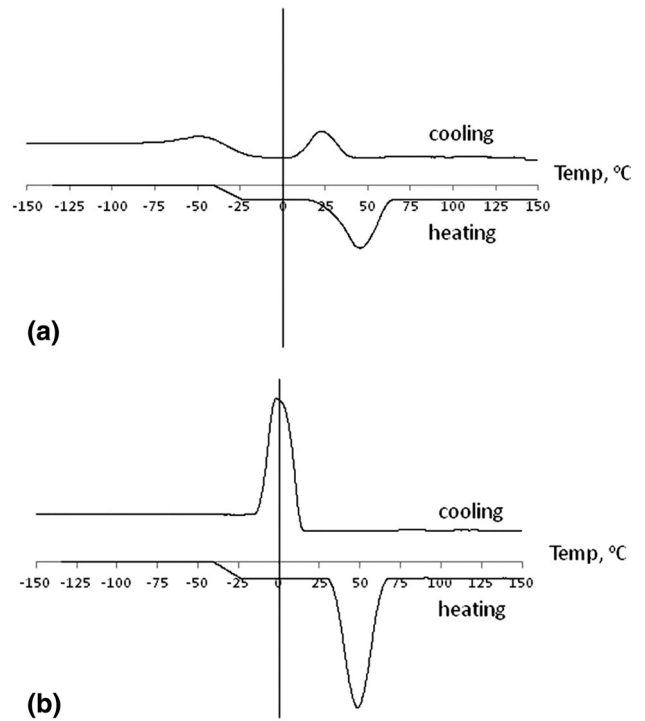


Fig. 6 DSC results of Ni-Ti thin film: (a) as-deposited, (b) with annealing at 650 °C for 30 min

same conditions and techniques as explained earlier. Figure 6(a) and (b) show the DSC results of as-deposited Ni-Ti thin film and that with annealing at 650 °C for 30 min, respectively. The results show that the transformation temperature of the annealed Ni-Ti thin film during heating and cooling was approximately close to room temperature, which was commonly found in Ni-rich NiTi alloy films (Ref 21, 26, 27). This result suggests that the majority of NiTi alloy material obtained from the annealing process at 650 °C for 30 min using the current preparation techniques is Ni-rich.

4. SMA Bimorph Actuator

After performing material characterization, annealing at 650 °C for 30 min at two pre-stressing conditions, i.e., a straight mold and curved mold, was chosen for the fabrication process of micro SMA bimorph actuators. Both molds, as shown in Fig. 2, were made of refractory concrete, and the curved mold had a radius of curvature around 22 mm. Figure 7 shows a bimorph SMA cantilever actuator. The actuators have two legs, $0.25 \times 22 \text{ mm}^2$, connected together with a $3 \times 3 \text{ mm}^2$ square pad at one end and a wire pad at the other. The copper was 12 μm thick and Ni-Ti thin film was 5 μm , similar to the samples in the previous section. The bimorph actuator with as-deposited Ni-Ti film bent convexly toward the Ni-Ti surface due to residual stress induced during the sputtering process. The radius of curvature of the bent actuators was around 50 mm. To create compressive strain on the Ni-Ti thin film during annealing, pre-stressing was applied by placing actuators in the refractory concrete molds in such a manner that the Ni-Ti film was facing upward.

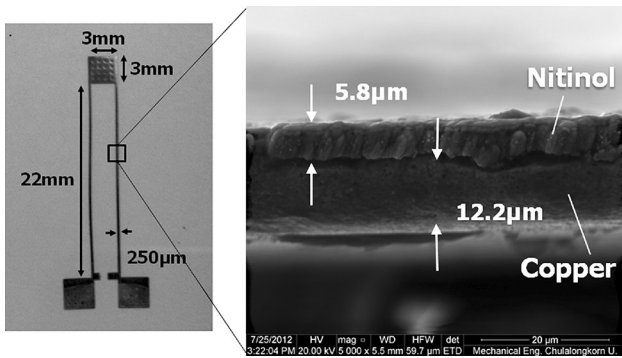


Fig. 7 Fabricated SMA bimorph actuator and its cross-section

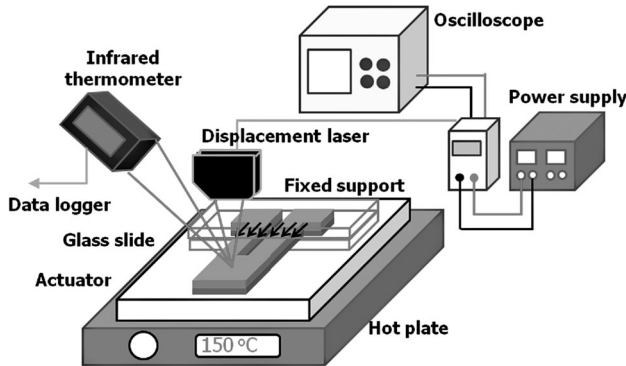


Fig. 8 Schematic of static response experimental setup

To investigate the effect of annealing conditions on the bimorph SMA actuator's performance, the deflection of three types of actuator, i.e., as-deposited Ni-Ti film and those with annealing in straight and curved molds, was examined in two manners, i.e., with static and dynamic responses. To install them to the test setup, they were clamped with glass slides by keeping the actuator length from its fixed end to tip at 22.5 mm, and the Ni-Ti thin film was kept toward the laser beam of a displacement sensor.

In the static response experiment, the deflection of the actuators was measured by the laser displacement sensor while using a hotplate to provide heat directly to the actuator structure. A schematic of this experimental setup is shown in Fig. 8. The temperature, which was controlled between 20 and 100 °C, was monitored using an infrared temperature sensor. The uncertainty of temperature measurement was around ± 1 °C while that of deflection was around ± 1 μm .

Figure 9(a)-(c) show the captured images of each actuator when their temperature was at room temperature and 90 °C, respectively. The average deflection of each actuator at different temperatures is shown in Fig. 10. The result shows that the annealed bimorph actuators provided larger deflection than that without annealing at the same actuating temperature. However, no significant difference for actuators with two pre-stressing conditions was observed. In addition, the deflection of all cases increased linearly with increasing actuator temperature. From experimental results, the deflection of the actuators without annealing and those with annealing in straight mold and curved mold was 0.57, 0.94, and 0.84 mm at 80 °C, respectively. Therefore, the annealing process significantly affected the

deflection of the NiTi-copper bimorph actuator, while the effect of pre-stressing condition on the deflection was relatively small.

In the dynamic response experiment, current was applied through the actuator's structure from one fixed end to the other. While the current passed through, heat was generated inside the actuator's structure as a result of the increasing temperature and bending of the structure. The deflection of the actuators while applying a square current signal to the actuators was examined using the laser displacement sensor. The amplitude of current signal was varied at 0.5, 0.75, 1.0, and 1.25 A, while its frequency was varied at 0.5, 1.0, and 2.5 Hz. This current signal was controlled and monitored using an amplifier and oscilloscope. The schematic of this experiment setup is shown in Fig. 11. Figure 12(a) and (b), respectively, show instantaneous deflection of the actuator with annealing in the straight and curved molds when applying different current amplitudes at the frequency of 0.5 Hz. For all annealing conditions including those without annealing (not shown), all actuators tended to respond immediately after applying and cutting off the current.

Figure 13 shows the summary of peak-to-peak deflection of these bimorph actuators at different applied current amplitudes at the frequency of 0.5 Hz. From the graph, the actuators deflected more largely when applying higher amplitude of current as expected. For example, the peak-to-peak deflection of actuator without annealing and with annealing inside the straight and curved molds at 1.25 A was 0.12, 1.7, and 1.3 mm, respectively.

The peak-to-peak deflection of the actuators when applying different driving frequencies at the current amplitude of 0.5 A is shown in Fig. 14. For lower driving frequency at fixed current amplitude, the peak-to-peak deflection became larger and vice versa. This was probably caused by the actuator being heated over a longer time duration at a lower driving frequency. Therefore, the temperature of the actuator's structure became higher, resulting in a larger peak-to-peak deflection in one cycle of the actuation. For example, the peak-to-peak deflection of the actuator that was annealed inside the straight mold decreased from 0.25 to 0.075 mm when the frequency was increased from 0.5 to 2.5 Hz.

Similar to the static response, the results show that there was a significant effect of the annealing temperature on the actuator's peak-to-peak deflection in the dynamic response experiment. On the other hand, the pre-stressing conditions had a relatively small effect.

5. Micro Gripper

The micro cantilever bimorph actuators were then applied as a micro gripper for small object manipulation. The configuration of the micro gripper is shown in Fig. 15. It consisted of two bimorph actuators and electric clamping. When current was applied, the gripper opened. After that, it was moved toward the position of a small object, and the gripper then grasped the object when the current was cut off. The holding was achieved due to an appropriate exerting force on the object. When the exerting force is high enough, it helps prevent the slipping down of the object. In this experiment, the micro gripper was tested to vertically grasp and hold objects with different weights to examine its lifting performance. Figure 16(a)-(d) show consecutively captured images of the micro gripper while

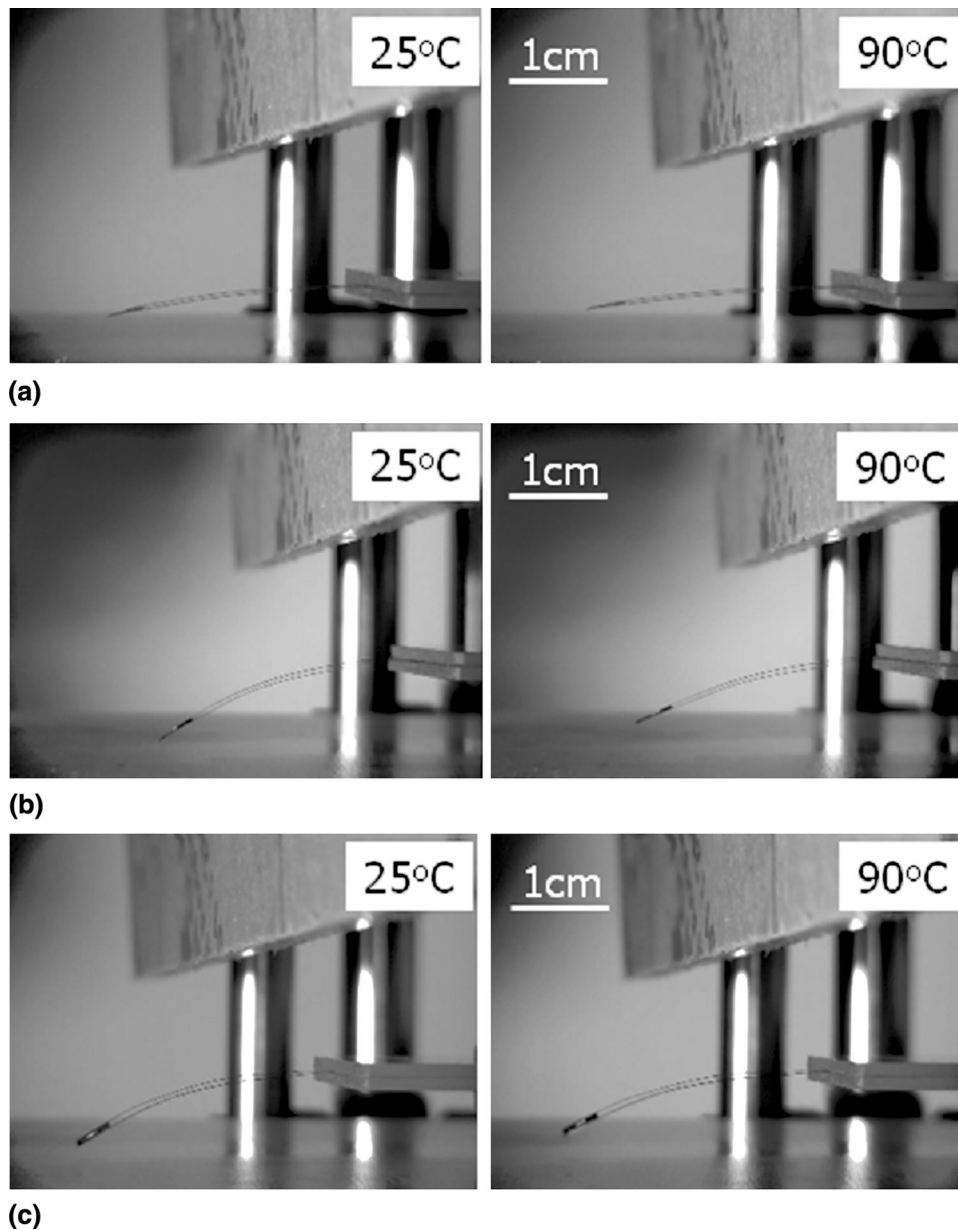


Fig. 9 Captured images of each actuator compared at room temperature and 90 °C: (a) without annealing, (b) annealed in a straight mold, (c) annealed in a curved mold

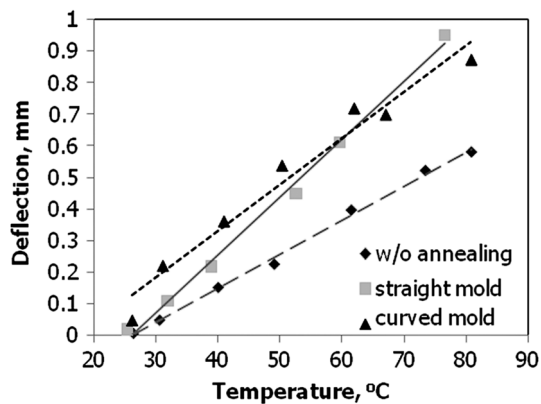


Fig. 10 Average static deflection of each actuator at different temperatures (two samples for each condition)

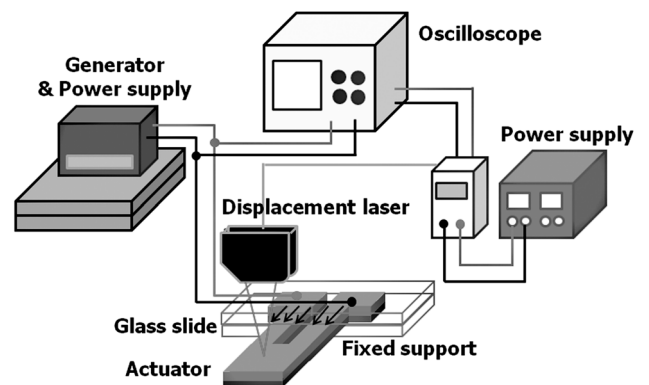


Fig. 11 Schematic of dynamic response experimental setup

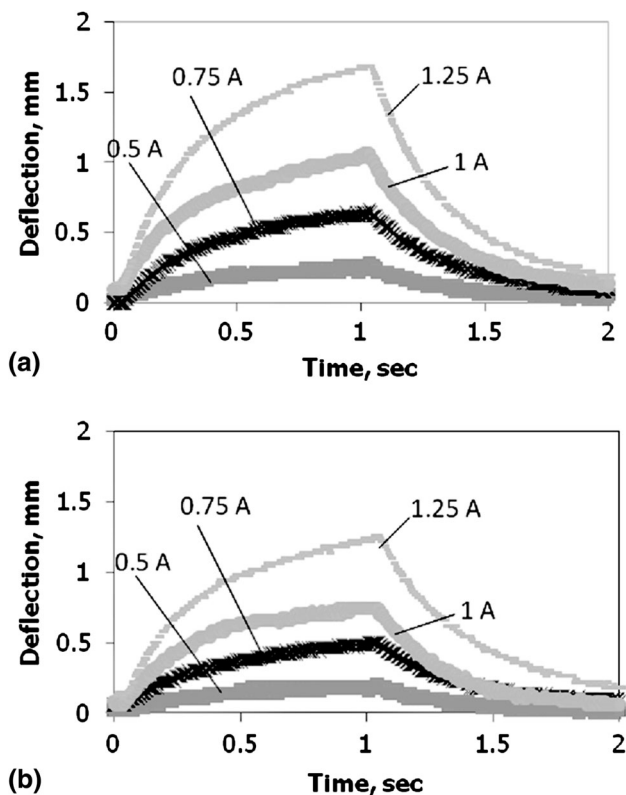


Fig. 12 Instantaneous responses when actuated using square current signal at different current amplitudes at a frequency of 0.5 Hz: (a) annealed in a straight mold, (b) annealed in a curved mold

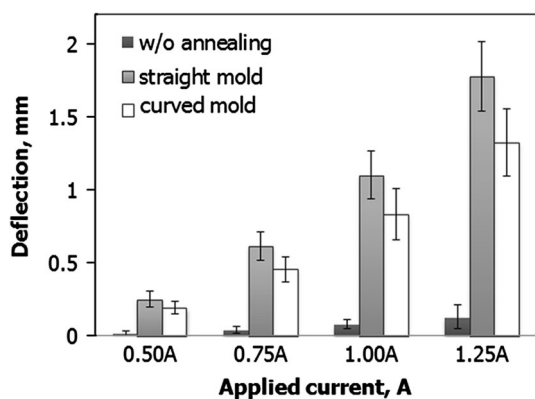


Fig. 13 Peak-to-peak deflection of each actuator at different current amplitudes at frequency of 0.5 Hz (two samples for each condition)

successfully grasping a small plastic ball which weighed 0.5 mg. Nevertheless, it was found that the micro gripper could not grasp and hold an object with a weight around 5 mg and over.

6. Conclusions

This paper presents a parametric study of the annealing process of Ni-Ti thin film on a copper substrate in a quartz tube

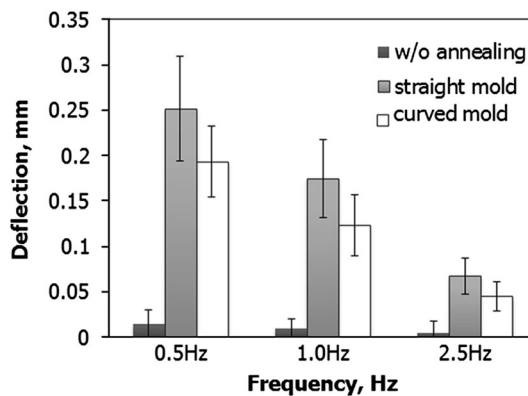


Fig. 14 Peak-to-peak deflection of each actuator at different driving frequencies at current amplitude of 0.5 A (two samples for each condition)

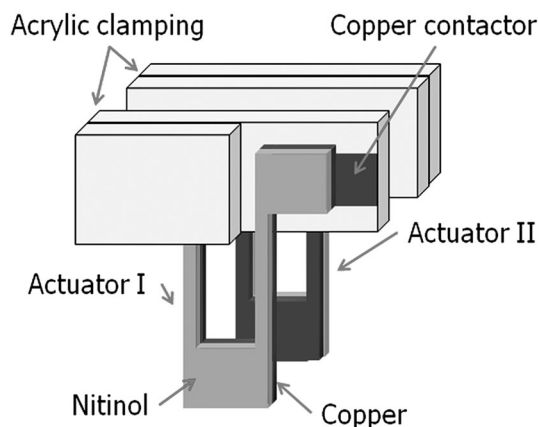


Fig. 15 Configuration of micro gripper assembled using two SMA bimorph actuators

furnace with argon overflow. The effect of annealing temperature, i.e., 500, 600 and 650 °C, for a duration of 30 min on the material characteristics was examined. After the actuator was fabricated, the effect of pre-stressing conditions, i.e., a straight mold and curved mold, on the actuator's deflection was then investigated. The following conclusions could be drawn. The annealing temperature strongly affected the formation of the crystalline structure of the Ni-Ti thin film. From this study, the appropriate temperature was higher than 600 °C where the NiTi crystalline structure started to orient properly. Moreover, at a higher annealing temperature, the NiTi crystalline structure oriented more completely, and the direct transformation from martensite to austenite phase was achieved when heated at 650 °C for 30 min. At high temperatures, the diffusion of copper and the formation of NiCu alloy structure were also observed. Moreover, oxide formation could not be avoided in the annealing technique employed in this study. At the end, the SMA bimorph actuator was successfully fabricated using the annealing conditions at 650 °C for 30 min. When comparing annealing temperature and pre-stressing conditions, the latter had less effect on the deflection of the bimorph actuator. Besides, the SMA bimorph actuator was successfully applied as a micro gripper for small object manipulation. From the study, the gripper could grasp and hold a small plastic ball with its weight of around 0.5 mg.

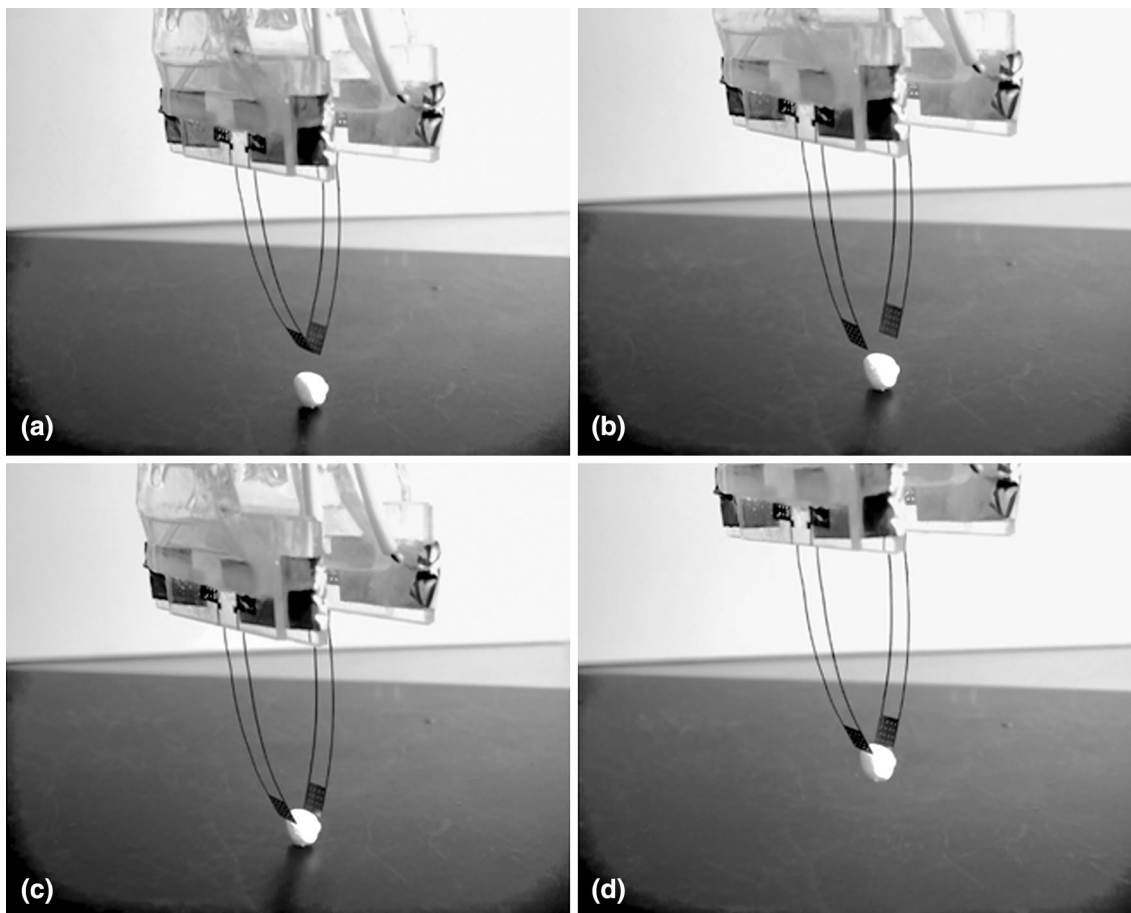


Fig. 16 Consecutively captured images of micro gripper while grasping a small plastic ball: (a) approaching, (b) opening, (c) grasping, (d) lifting, and holding

Acknowledgment

This research was financially supported by the 90th Anniversary of Chulalongkorn University Fund (Ratchadaphiseksomphot Endowment Fund) and Special Task Force for Activating Research (STAR) of Chulalongkorn University, Thailand through the Micro-Nano Fabrication Technology Research Group (GSTAR 56-005-21-002). In addition, the authors would like to thank Dr. Anurat Wisitorsaat (Microelectronics and MEMS laboratory, NECTEC) and Dr. Tachai Luangvaranunt (Department of Metallurgical Engineering, Chulalongkorn University) for their assistance in sample preparation.

References

1. P. Krulevitch, A.P. Lee, P.B. Ramsey, J.C. Trevino, J. Hamilton, and M.A. Northrup, Thin Film Shape Memory Alloy Microactuators, *J. Microelectromechanical Syst.*, 1996, **5**(4), p 270–282
2. S. Miyazaki and A. Ishida, Martensitic Transformation and Shape Memory Behavior in Sputter-Deposited TiNi-Base Thin Films, *Mater. Sci. Eng.*, 1999, **A273–275**, p 106–133
3. W. Huang, On the Selection of Shape Memory Alloys for Actuators, *Mater. Des.*, 2002, **23**, p 11–19
4. B. Winzek, S. Schmitz, H. Rumpf, T. Sterzl, R. Hassdorf, S. Thienhaus, J. Feydt, M. Moske, and E. Quandt, Recent Developments in Shape Memory Thin Film Technology, *Mater. Sci. Eng. A*, 2004, **378**, p 40–46
5. Y. Fu, H. Du, W. Huang, S. Zhang, and M. Hu, TiNi-Based Thin Films in MEMS Applications: A Review, *Sens. Actuators A*, 2004, **112**, p 395–408
6. Y. Bellouard, Shape Memory Alloys for Microsystems: A Review from a Material Research Perspective, *Mater. Sci. Eng. A*, 2008, **481–482**, p 582–589
7. L. Fumagalli, F. Butera, and A. Coda, SmartFlex[®] NiTi Wires for Shape Memory Actuators, *J. Mater. Eng. Perform.*, 2009, **18**, p 691–695
8. M. Frotscher, F. Kahleyss, T. Simon, D. Biermann, and G. Eggeler, Achieving Small Structures in thin NiTi Sheets for Medical Applications with Water Jet and Micro Machining: A Comparison, *J. Mater. Eng. Perform.*, 2011, **20**, p 776–782
9. Y.H. Li, M.K. Li, F.L. Meng, and W.T. Zheng, Investigation on Mechanical Properties of Deformation TiNi Thin Films, *J. Mater. Eng. Perform.*, 2012, **21**, p 2691–2694
10. K. Lygin, S. Langbein, P. Labenda, and T. Sadek, Methodology for the Development, Production and Validation of R-Phase Actuators, *J. Mater. Eng. Perform.*, 2012, doi:10.1007/s11665-012-0285-1
11. E. Makino, T. Mitsuya, and T. Shibata, Fabrication of TiNi Shape Memory Micropump, *Sens. Actuators A*, 2001, **88**, p 256–262
12. F. Sassa, Y. Al-Zain, T. Ginoza, S. Miyazaki, and H. Suzuki, Miniaturized Shape Memory Alloy Pumps for Stepping Microfluidic Transport, *Sens. Actuators B*, 2012, **165**, p 157–163
13. S. Takeuchi and I. Shimoyama, A Three-Dimensional Shape Memory Alloy Microelectrode with Clipping Structure for Insect Neural Recording, *J. Microelectromechanical Syst.*, 2000, **9**(1), p 24–31
14. J.J. Gill, D.T. Chang, L.A. Momoda, and G.P. Carman, Manufacturing Issues of Thin Film NiTi Microwrapper, *Sensors Actuators A*, 2001, **93**, p 148–156

15. Y.Q. Fu, J.K. Luo, S.E. Ong, S. Zhang, A.J. Flewitt, and W.I. Milne, A Shape Memory Microcage of TiNi/DLC Films for Biological Applications, *J. Micromech. Microeng.*, 2008, **18**(3), p 035026
16. C.Y. Chung and P.M. Chan, NiTi Shape Memory Alloy Thin Film Micro-cantilevers Array, *Thin Solid Films*, 2011, **519**, p 5307–5309
17. X. Wang, Y. Bellouard, and J.J. Vlassak, Laser Annealing of Amorphous NiTi Shape Memory Alloy Thin Films to Locally Induce Shape Memory Properties, *Acta Mater.*, 2005, **53**, p 4955–4961
18. Y. Motemani, M.J. Tan, T.J. White, and W.M. Huang, Rapid Thermal Annealing of Ti-Rich TiNi Thin Films: A New Approach to Fabricate Patterned Shape Memory Thin Films, *Mater. Des.*, 2011, **32**, p 688–695
19. A. Pimpin, E. Wongweerayoot, and W. Srituravanich, Two-Step Electroplating Process in Fabrication of Thermal Bimorph Cantilever Actuator for Flow Control Application, *Appl. Mech. Mater.*, 2012, **225**, p 367–371
20. K.T. Liu and J.G. Duh, Hardness Evolution of NiTi and NiTiAl Thin Films Under Various Annealing Temperatures, *Surf. Coat. Technol.*, 2008, **202**, p 2737–2742
21. S. Sanjabi and Z.H. Barber, The Effect of Film Composition on the Structure and Mechanical Properties of NiTi Shape Memory Thin Films, *Surf. Coat. Technol.*, 2010, **204**, p 1299–1304
22. A. Kumar, S.K. Sharma, S. Bysakh, S.V. Kamat, and S. Mohan, Effect of Substrate and Annealing Temperatures on Mechanical Properties of Ti-Rich NiTi Films, *J. Mater. Sci. Technol.*, 2010, **26**(11), p 961–966
23. G.S. Firstov, R.G. Vitchev, H. Kumar, B. Blanpain, and J. Van Humbeeck, Surface Oxidation of NiTi Shape Memory Alloy, *Biomaterials*, 2002, **23**, p 4863–4871
24. A. Undisz, R. Hanke, and M. Rettenmayr, Effect of Heating Rate on Surface Composition of Annealed NiTi, *Shape Memory and Superelastic Technologies*, Prague, Czech Republic, 2013
25. D. Vojtěch, M. Voděrová, J. Fojt, P. Novák, and T. Kubásek, Surface Structure and Corrosion Resistance of Short-Time Heat-Treated NiTi Shape Memory Alloy, *Appl. Surf. Sci.*, 2010, **257**, p 1573–1582
26. P. Surbled, C. Clerc, B. Le Pioufle, M. Ataka, and H. Fujita, Effect of the Composition and Thermal Annealing on the Transformation Temperatures of Sputtered TiNi Shape Memory Alloy Thin Films, *Thin Solid Films*, 2001, **401**, p 52–59
27. J. Khalil-Allafi, G. Eggeler, A. Dlouhy, W.W. Schmahl, and C. Somsen, On the Influence of Heterogeneous Precipitation on Martensitic Transformations in a Ni-Rich Shape Memory Alloy, *Mater. Sci. Eng. A*, 2004, **378**, p 148–151